DOI: 10.1002/ejic.200800724

Nonheme "$Fe^{IV}O$" Models: Ab Initio Analysis of the Low-Energy Spin State Electronic Structures

Frédéric Banse,*[a] Jean-Jacques Girerd,[a] and Vincent Robert*[b]

Keywords: Metalloenzymes / Spin states / Ab initio calculations / Spin crossover / Iron

The spin-dependent geometries, energetics, and electronic structures of the $[FeO]^{2+}$ motif are investigated on the basis of DFT and perturbative CASPT2 ab initio calculations. The synthetic complex $[(L_5^2)FeO]^{2+}$ exhibits an $S = 1$ ground state with a low-lying (≈2000 cm^{-1}) competing quintet and an open-shell singlet as the second excited state (≈11000 cm^{-1} above the ground state). By using the geometry optimization information, it was shown from a valence bond reading of the variational wavefunctions that a Fe^{III}–$O^{\cdot}$ picture dominates and that the number of d electrons is almost five in the model system $[Fe(NH_3)_5O]^{2+}$. Analogy with the spin-crossover transition phenomenon is suggested, as the ground and low-lying quintet states can be seen as resulting from a doublet → quartet transition of a Fe d^5 ion.

Introduction

Many metalloenzymes use iron as a cofactor to carry out specific oxidation reactions.[1] It has long been invoked that the intermediates responsible for the target reactions were high valent iron–oxido intermediates.[2–5] Thus, chemists have made efforts to prepare models of these high-valent Fe species, primarily focusing on the Fe–oxygen motif. Regarding the formally Fe^{IV} family of mononuclear nonheme enzymes, high-spin ($S = 2$) Fe^{IV}–oxido compounds have been identified in taurine/α-ketoglutarate dioxygenase (TauD)[6] and more recently in prolyl-4-hydroxylase (P4 H)[7] and halogenase CytC3.[8] Conversely, synthetic models that have been reported so far contain low-spin ($S = 1$) centers,[2,9] with the single exception of the in situ generated $[(H_2O)_5Fe^{IV}O]^{2+}$ ion.[10] In contrast to TauD, which specifically catalyzes hydroxylation of taurine,[11] the oxidation of alkanes with nonactivated C–H bonds (e.g., cyclohexane) by synthetic models has been reported in a few cases but generally yields products deriving from radical chain reactions.[9,12] It has been inferred from density functional theory (DFT) calculations that the nature of the Fe=O bond remains almost the same in the two spin states.[13] Nevertheless, Shaik et al. have shown that C–H activation by nonheme Fe^{IV}–oxido models may be rationalized by so-called two-state reactivity (TSR)[14] due to the proximity of the ground state $S = 1$ and the excited state $S = 2$.[15,16] After H-abstraction, the ground state $S = 1$ surface displays a barrier for the radical rebound, whereas this step is a lower-energy pathway or barrier free in the $S = 2$ state. Then, products deriving from radical rearrangements are indeed expected if the triplet state participates in the reaction.[15,16] DFT calculations performed on models of the TauD Fe^{IV}–oxido intermediate have recently demonstrated that relatively small changes in the coordination sphere involving the binding mode of the carboxylates is likely to tune the ground-state spin multiplicity (i.e., $S = 2$ vs. $S = 1$).[17] However, as mentioned by the authors,[17] uncertainties in the determination of the spin-state energetics are intrinsic to DFT methods.[18]

From the experimental point of view, Mössbauer spectroscopy is a powerful tool to investigate this class of compounds. Because the isomer shift and quadrupole splitting are sensitive to subtle changes in the electronic structure, these parameters might be insightful to the environment of the iron ion.[17,19,20] Indeed, oxidation numbers and spin states can have major effects in Mössbauer isomer shift values. However, the distinction between $S = 1$ Fe^{III} and $S = 1$ or 2 Fe^{IV} may not be directly accessible.[21] Not only does the concept of formal oxidation number remain unadapted, but the importance of charge transfers may greatly modify this limiting picture. The assignment of oxidation numbers is a frequently encountered issue in all areas of chemistry, as recently illustrated for iron oxides.[22]

In the course of our investigations of high-valent Fe–oxido intermediates, we synthesized and identified $[FeO]^{2+}$ complexes with neutral ligands of the L_5^2 family [cf. Scheme 1, L_5^2 = *N*-methyl-*N*,*N*′,*N*′-tris(2-pyridylmethyl)-ethane-1,2-diamine].[9,23]

[a] Institut de Chimie Moléculaire et des Matériaux d'Orsay, Laboratoire de Chimie Inorganique, Université Paris Sud 11
91405 Orsay Cedex, France
Fax: +33-1-69154754
E-mail: fredbanse@icmo.u-psud.fr
[b] Laboratoire de Chimie, Ecole Normale Supérieure de Lyon
46, allée d'Italie 69364 Lyon cedex07, France
Fax: +33-4-72728860
E-mail: vrobert@ens-lyon.fr

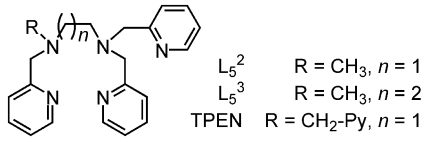

Scheme 1. Structure of ligands of the L_5^2 family used for the generation of $[FeO]^{2+}$ complexes.

None of the molecular structures were resolved for these complexes. Nevertheless, there is strong experimental evidence that supports an $S = 1$ ground state in these systems. On the basis of several theoretical studies, it has been proposed,[23–25] and later refuted,[13,26] that these species could be best described as Fe^{III}–$O^{\cdot}$ rather than Fe^{IV}=O (see Scheme 2).[23] This description could explain the interesting activity of these intermediates towards the oxidation of *cis*-stilbene that yielded the *trans*-epoxide preferentially.[9,23] To which extent these $S = 1$ synthetic systems as opposed to $S = 2$ natural ones may be promising catalytic targets is a challenging theoretical question.

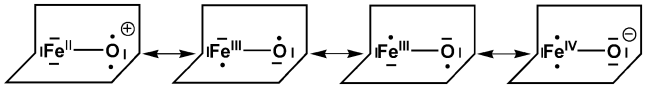

Scheme 2. Mesomer forms of the $[FeO]^{2+}$ motif.

From a theoretical point of view, the zero overlap model does not hold to describe such short Fe–O distances (ca. 1.65 Å),[27,28] Complete active space self-consistent field (CASSCF) simulations do not properly account for charge fluctuations,[23] whereas DFT calculations may suffer from the unadapted single determinantal description of open-shell systems.[29] Besides, this method suffers from the arbitrariness of the exchange correlation functional and the somewhat overestimated delocalization character of the orbitals. Because the Fe-3d and O-2p atomic orbitals (AOs) are strongly mixed, one expects important charge transfers that are to be quantified. Starting from the standard Fe^{IV}=O picture, single and double charge-transfer forms Fe^{III}–$O^{\cdot}$ and Fe^{II}–O^{+} (cf. Scheme 2) are expected to contribute to the different spin state electronic structures. Even though agreement has been reached as to the spin density splitting between the Fe and O atoms for nonheme models with neutral ligands,[13,23,24,26] significant variations in the spin populations of the speculated $S = 1$ TauD Fe^{IV}–oxido intermediate have been recently reported, ranging from 1.23/0.84 to 1.53/0.50 on Fe and O, respectively.[17]

Therefore, we felt that a detailed inspection of the $[FeO]^{2+}$ fragment would be very helpful to clarify (i) the electronic structure and low-energy states of our synthetic $[FeO]^{2+}$ motif $[(L_5^2)FeO]^{2+}$ (**1**; cf. Figure 1),[9,23] (ii) the electronic distribution in the Fe=O bond in terms of Fe^{II}, Fe^{III}, and Fe^{IV} forms, and (iii) the $S = 1$, $S = 2$, and competing $S = 0$ electronic structures as the Fe–O distance is varied in model compound $[Fe(NH_3)_5O]^{2+}$ (**2**; cf. Figure 1). With this goal in mind, orthogonal relocalized CASSCF MOs were used to perform a valence-bond-type analysis of the wavefunction.

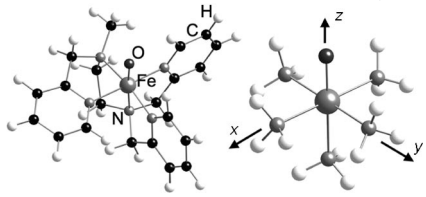

Figure 1. Structures of **1** $[(L_5^2)FeO]^{2+}$ (left) and of model compound **2** $[Fe(NH_3)_5O]^{2+}$ (right).

Thus, DFT and wavefunction-based ab initio calculations were performed to investigate the character of these spin states in terms of the Fe^{II}, Fe^{III}, and Fe^{IV} contributions (see Scheme 2). Because of the lack of X-ray diffraction data, necessary structural information was first extracted from DFT geometry optimizations. Then, nonvertical transition energies and electronic distributions available in the wavefunctions of both **1** and model compound **2** (see Figure 1) were investigated by CASSCF calculations and subsequent second-order perturbation theory (CASPT2). Finally, a detailed inspection based on variational CAS+ single calculations was carried out to analyze the charge reorganization phenomena.

Results and Discussion

Spin-State Energetics of 1

Full DFT geometry optimizations were performed on **1** in the different spin states ($S = 0$, $S = 1$, $S = 2$; cf. Table 1) by using both B3LYP and BP86 functionals. Standard Fe–N and Fe–O bond lengths are observed whatever the functional. The major structural changes between the $S = 1$ and the $S = 2$ states are, as expected in spin-transition systems,[30] the increase in the Fe–N_{eq} equatorial bond lengths. Nevertheless, the bond length change (≈0.1 Å) is about twice as small as that in the traditional singlet → quintet Fe^{2+} spin-crossover (SCO) systems.[31] In contrast, the Fe–N_{ax} axial and Fe–O bond lengths are almost unaffected. The ligand-field effect was already analyzed as the spin state changes from $S = 1$ to $S = 2$.[13,26] Interestingly, the $S = 1$ and $S = 0$ structures are very similar with bond length changes of ca. 2%. Finally, the spin-states energies calculated by using the corresponding optimized geometries (i.e., adiabatic transition) leave $S = 1$ as the ground state and $S = 2$ and $S = 0$ lying at 2300 and 11300 cm^{-1} above, respectively.

Table 1. Structural data obtained by DFT for **1** in the $S = 1$ ground state and in the two excited states $S = 2$ and $S = 0$.

$[(L_5^2)FeO]^{2+}$ (**1**)	Fe–O [Å]	Fe–N_{ax} [Å][a]	Fe–N_{eq} [Å][b]
$S = 1$	1.65	2.12	2.02
$S = 2$	1.64	2.14	2.14
$S = 0$	1.65	2.12	2.04

[a] N_{ax} represents the axial N ligand. [b] Average distance between Fe and the equatorial N_{eq} ligands.

Because DFT calculations are known to overestimate charge delocalization, wavefunction-based calculations were also performed. Therefore, demanding ab initio CAS(14,15)-SCF calculations including 14 electrons in 15 molecular orbitals (MOs) and subsequent CASPT2 treatment were carried out by using the DFT-optimized spin-dependent geometries for **1**. This particular active space includes an extra set of 3d orbitals in order to properly account for the d electron correlation energy at the CASSCF level.[32,33] The importance of the so-called 3d′ set was reported in the spectroscopic analysis of spin-transiting systems.[34] As in most synthetic models studies, our results show that the ground state is triplet (S = 1), whereas the excited quintet (S = 2) state is found in a close proximity at ca. 1200 cm^{-1} above. This result is in reasonably good agreement with the value obtained by DFT calculations (2300 cm^{-1}). These consistent CASPT2 and DFT calculation results rule out the possibility to use such a neutral amine/pyridine environment to favor the biologically relevant S = 2 over the S = 1 state. A synthetic strategy to reverse the spin-state ordering would be to modify the equatorial ligand field. With this goal in mind, one may either use stronger π-donors in the equatorial plane[26] or bulkier ligands.[26,35] Finally, the open-shell singlet (S = 0) previously reported[36] is found higher in energy: 11000 cm^{-1} above the triplet state. Because the S = 0 and S = 1 geometries are not rigorously identical, these excitation energies are not strictly Franck–Condon transitions. The triplet-singlet energy difference we found by using DFT and CASPT2 calculations turned out to be twice as large as those previously reported for similar compounds.[36]

Microscopic Analysis of the Fe–O Bond in 2

The efficiency of such formal $[FeO]^{2+}$ motifs in achieving an oxidation reaction strongly depends on the Fe=O bonding nature[37] and spin state. However, what might be a relevant configuration assignment to such $[FeO]^{2+}$ species has not been completely unraveled. In particular, how much should the traditional Fe^{IV}=O[13,21] configuration picture $(d_{xy})^2(d_{xz})^1(d_{yz})^1$ be favored over Fe^{III}–$O^{\cdot}$[23,24] as π covalency competes with electron correlation effects? In order to scrutinize the nature of the Fe=O motif giving rise to a variety of competing spin states, we focused on the electronic description of a simplified model in which the critical Fe–O distance was varied. This particular model system **2** (cf. Figure 1) turned out to be a relevant surrogate to investigate this class of compounds.[23,26] Therefore, we performed a systematic theoretical analysis of the S = 0, S = 1, and S = 2 spin state electronic structures of model system **2**.

Our goal was to evaluate the weights of the different electronic configurations shown in Scheme 2. At this stage, a smaller active space [CAS(10,8)] was chosen to perform a systematic wavefunction analysis concentrated on the frontier MOs (cf. Figure 2). These MOs are built from a naive Fe^{4+}/O^{2-} picture. Nevertheless, owing to their important delocalization character, one may wonder how much the electronic spin density is split between the Fe and O atoms.

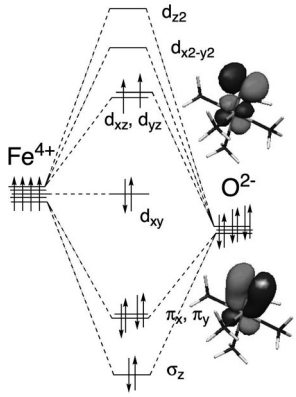

Figure 2. S = 1 valence MOs used in the CAS(10,8)SCF+ single variational calculations. Only one set of the degenerate (π_x,π_y) and (π_x*,π_y*) orbitals is shown.

On the basis of the geometry optimizations of **1**, the $Fe–N_{eq}$ and $Fe–N_{ax}$ bonds were fixed by using the spin-dependent Fe–N and Fe–O bond lengths given in Table 1. The use of an average $Fe–N_{eq}$ value (C_{4v} symmetry) allowed us to simplify the wavefunction reading. Starting from the equilibrium Fe–O distance (1.65 Å) defining the z axis, this bond was contracted to 1.45 Å or elongated to 1.85 Å to investigate the charge reorganization. Nevertheless, the analysis of the multireference wavefunction in terms of the CASSCF MOs was not straightforward, as both the CI expansion and the delocalized MOs incorporate information upon covalency. Starting from the intuitive Fe^{IV}=O picture, one may look into the charge fluctuation configurations to estimate the d-orbital occupancy. Thus, the relevant CASSCF π-active orbitals were relocalized either on the Fe or O center to grasp the investigated information in the CI expansion only (cf. Figure 3). The relocalized orbitals, which will be used throughout the following wavefunction analysis, exhibit large atomic character. Let us stress that the two sets of MOs differ by a unitary transformation within the active space. Such a rotation maximizes the weights of the d and p atomic orbitals on the Fe and O centers, respectively. This transformation leaves any observable expectation value unchanged (in particular, the energy). Nevertheless, the atomic-like orthogonal MOs (i.e., relocalized MOs) offer a charge-transfer decomposition of the wavefunction. It was recently shown that such decomposition of the CASSCF wavefunction allows one to grasp its physical content in terms of the possible distributions of the valence electrons in molecularly optimized atomic-like orthogonal orbitals.[38] By using the resulting relocalized orbitals, the energetics and character of the lowest S = 0, 1, and 2 states of model system **2** were evaluated at a CAS+ single level.[39]

Our results are summarized in Table 2. By varying the Fe–O distance, we find that the ground-state triplet is largely dominated (≈65%) by the charge-transfer Fe^{III}–$O^{\cdot}$ configuration. By using the correlated S = 0, S = 1, and S = 2 wavefunctions, the weights of the Fe^{II}, Fe^{III}, and Fe^{IV} forms were calculated. The average Fe-3d orbitals occupa-

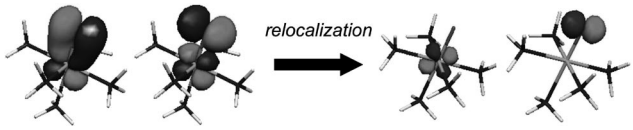

Figure 3. Delocalized and relocalized valence triplet orbitals of **2**. A similar set is obtained in the perpendicular plane.

tion ($\bar{d}$) was simply evaluated by weighting the corresponding six-, five-, and four-electron forms. This value remains almost unchanged, and close to five, in the three spin states, whatever the Fe–O probed distance. A detailed inspection shows that the Fe^{IV}/Fe^{II} ratio drastically decreases as the bond length increases in the $S = 0$ and $S = 1$ states, whereas this value is much less sensitive in the $S = 2$ state. Furthermore, the Fe^{III}–$O^{\cdot}$ and Fe^{IV}=O forms always contribute to ca. 80% in the latter. In contrast to the $S = 2$ state, the ground $S = 1$ and $S = 0$ states exhibit a nonnegligible O → Fe charge transfer in the long-distance regime.

Table 2. Relative contributions [%] of the Fe^{II}, Fe^{III}, and Fe^{IV} forms for **2** and average Fe-3d atomic-like orbital occupation ($\bar{d}$).

Fe–O [Å]	1.45	1.65	1.85
$S = 1$ / $\bar{d}$	15:61:24 / 4.9	13:67:20 / 4.9	28:68:04 / 5.2
$S = 2$ / $\bar{d}$	18:61:21 / 5.0	18:64:18 / 5.0	22:66:12 / 5.1
$S = 0$ / $\bar{d}$	13:67:20 / 4.9	13:77:10 / 5.0	13:83:04 / 5.1

In light of the ab initio calculations, a $(d_{xy})^2(d_{xz},d_{yz})^3$ configuration is favored in the $S = 1$ and $S = 0$ states. As a result of the orthogonality of the d_{yz} (respectively, d_{xz}) and p_x (respectively, p_y) orbitals, the ground state is triplet (Hund's rule) and consists of an equal weight of the $(d_{yz})^1(p_x)^1$ and $(d_{xz})^1(p_y)^1$ triplet configurations. Even though the involved AOs are (i) different in nature (2p in O_2, 2p/3d in FeO) and (ii) degenerate in O_2, nondegenerate in the $[FeO]^{2+}$ motif, the constitutions of the MOs in the $S = 0$ and $S = 1$ states are very similar in both the O_2 and $[FeO]^{2+}$ systems.[25] Let us mention that this kinship was suggested for late-transition-metal oxido bonds MO^+.[40,41] As expected, the singlet state is reminiscent of the Δ singlet of the O_2 molecule.[42] In particular, the rather delocalized character of the MOs already reported in $[FeO]^{2+}$ complexes[9,14,15,17] strengthens this analogy and the preference for the $(d_{xy})^2(d_{xz},d_{yz})^3$ configuration over the $(d_{xy})^2(d_{xz},d_{yz})^2$ configuration. Thus, the Fe spin character should be considered as doublet in the $S = 0$ and 1 spin states of the $[FeO]^{2+}$ motif.

This is in contrast to the low-lying $S = 2$ spin state. The formally nonbonding d_{xy} → antibonding $d_{x^2-y^2}$ promotion leads to a $(d_{xy})^1(d_{xz},d_{yz})^3(d_{x^2-y^2})^1$ configuration and an intermediate spin-state quartet on Fe results. Because the $S = 1 \rightarrow S = 2$ conversion only implies orbitals lying in the equatorial plane (i.e., d_{xy}, perpendicular to the Fe–O bond), this picture is compatible with the spin independence of the Fe–O distance as previously reported.[13,26] On the basis of our wavefunction analysis, the net $S = 1 \rightarrow S = 2$ phenomenon should be seen as a doublet → quartet spin transition occurring on the Fe center. Such a picture explains the structural changes accompanying the SCO phenomenon. By using a monoelectronic picture, the number of promoted electrons in the traditionally studied singlet → quintet transition is twice the number in the present doublet → quartet phenomenon. This conclusion is consistent with the reduction of the Fe–N_{eq} bond lengths in **1**. Let us stress that such an analysis holds for Fe^{IV}=O, for which a triplet → quintet transition on Fe must be considered. Finally, spin-density analysis shows that the Fe=O bond exhibits a 1/1 and 3/1 splitting in the $S = 1$ and $S = 2$ states, respectively. These values are in relatively good agreement with previous DFT-based analyses.[13,24,26] Interestingly, these values are almost unaffected as the bond length changes.

Conclusions

DFT calculations were performed on $[(L_5^2)FeO]^{2+}$, a complex we had previously reported but not structurally characterized.[23] The geometry optimizations allowed us to perform low-lying spin state spectroscopy by using both DFT and CASPT2 calculations. The geometries of each spin state were fully optimized and almost identical for the $S = 0$ and $S = 1$ states, whereas the $S = 2$ state exhibits a ca. 0.1 Å elongation in the Fe–N distances in the equatorial plane. The ground state was found to be triplet. The competing quintet lies ≈2000 cm^{-1} above the ground state, whereas the open-shell singlet was found to be much higher in energy. Starting from this structural information, variational wavefunction ab initio calculations were performed on a model $[Fe(NH_3)_5O]^{2+}$ system to obtain a detailed description of the Fe=O bond in $[FeO]^{2+}$-based complexes. On the basis of valence-bond-type reading of the wavefunction, our calculations show that starting from the ionic picture Fe^{4+}/O^{2-}, the O → Fe charge transfer leads to an average number of d electrons of five on Fe in the three-spin states. Low-lying spin state spectroscopy in such system can be seen as resulting from a doublet → quartet spin transition on the Fe center. Let us mention that even though the dominating configuration in the $S = 2$ spin state is consistent with an Fe quartet, a nonnegligible Fe^{IV}=O character subsists, whatever the Fe–O distance. Finally, an interesting kinship between the electronic structures of O_2 and $[FeO]^{2+}$, with six π electrons in four MOs (cf. Figure 2) was found. In particular, the presence of an $[FeO]^{2+}$ singlet, reminiscent of the Δ singlet of the O_2 molecule, can be looked for, as the latter is known to be a strong oxidizing agent for organic substances. If accessible, the $[FeO]^{2+}$ singlet looks like a promising candidate for oxidation reactions.

Computational Details

The synthesis of $[L_5^2FeO]^{2+}$ (**1**) was described previously,[23] but no structural information was reported. Thus, the geometry of each spin state was fully optimized at the unrestricted UB3LYP level by using standard basis set 6-311G. Such a hybrid functional has proven to provide very satisfactory results.[43] Relativistic corrections do not lead to any significant changes in the bond lengths.

For single-point energy calculations, a 6-311G* basis set was used. All our DFT calculations were performed with the use of the Gaussian 03 program.[44] The sensitivity of the geometries and energetics with respect to the functional were evaluated on the basis of complementary UBP86/6-311G calculations. Regarding the multireference calculations, we used the CASSCF approach and CASPT2 treatment as implemented in the MOLCAS 5.4 package.[45] The one-electron basis sets employed in the present work to describe the MOs were derived from 21s15p10d6f4g primitive functions contracted into 5s5p3d1f for Fe, 10s6p3d into 3s3p1d for O and N atoms, and 3s into 1s for H. Carbon atoms were described with smaller basis sets (i.e., double zeta) to reduce the computational cost for calculations on **1**.

In order to grasp the underlying physical phenomena, complementary wavefunction-based calculations were performed. Along the CASSCF scheme, one qualitatively introduces in a multireference wavefunction the leading physical configurations in the different states of interest performing a full configurations interaction (CI) within a limited space referred to as the complete active space (CAS). The resulting *n*-electron wavefunction is formed by linear combination of the so-called Slater determinants. Considering the speculated electronic structure, the CAS we chose consists of 14 electrons (4 d, 6 p, and 2 s electrons arising from the $Fe^{IV}O$ reference configuration, and one e_g-type bonding pair on the equatorial part of the ligand) in 15 MOs [5 mainly d-type centered on Fe, 4 arising from the oxygen valence orbitals, one bonding e_g-type, and an extra set of d-type orbitals, CAS(14,15)]. The latter set (so-called double-shell) accounts for the radial correlation effects within the iron 3d shell.[33] A different active space was used previously that did not include a second set of 3d orbitals.[26] This choice of active space ensures a balanced treatment of the most important electronic configurations $Fe^{IV}O$, $Fe^{III}O^{\cdot}$, and $Fe^{II}O^{+}$. The CASSCF method allows one to account for nondynamic correlation effects. Nevertheless, it fails to reproduce the transition energies because of the lack of dynamical correlation contributions. In order to incorporate such physical effects, CASPT2 calculations were carried out by using an imaginary shift of 0.3 Hartree to avoid the presence of intruder states.[22] All electrons, except the core ones (1s for O and N; 1s, 2s, and 2p for Fe), were correlated. Even though greatly demanding, these calculations allow one to evaluate non Franck–Condon transition energies. CAS+ single variational calculations were also performed on a smaller active space [CAS(10,8)], as we were mostly interested in examining the charge redistribution on the FeO moiety. This CAS corresponds to the Fe-3d and O-2p sets occupied by 10 electrons.

Acknowledgments

The Institut du Développement et des Ressources en Informatique Scientifique (IDRIS) is acknowledged for support.

[1] S. J. Lippard, J. M. Berg, *Principles of Bioinorganic Chemistry*, University Science Books, Mill Valley, **1994**, p. 302–318.
[2] M. Costas, M. P. Mehn, M. P. Jensen, L. Que Jr., *Chem. Rev.* **2004**, *104*, 939–986.
[3] E. I. Solomon, T. C. Brunold, M. I. Davis, J. N. Kemsley, S.-K. Lee, N. Lehnert, F. Neese, A. J. Skulan, Y.-S. Yang, J. Zhou, *Chem. Rev.* **2000**, *100*, 235–349.
[4] M. Sono, M. P. Roach, E. D. Coulter, J. H. Dawson, *Chem. Rev.* **1996**, *96*, 2841–2887.
[5] Y. Watanabe, H. Nakajima, T. Ueno, *Acc. Chem. Res.* **2007**, *40*, 554–562.
[6] P. J. Riggs Gelasco, J. C. Price, R. B. Guyer, J. H. Brehm, E. W. Barr, J. M. Bollinger Jr., C. Krebs, *J. Am. Chem. Soc.* **2004**, *126*, 8108–8109.
[7] L. M. Hoffart, E. W. Barr, R. B. Guyer, J. M. Bollinger Jr., C. Krebs, *Proc. Natl. Acad. Sci. USA* **2006**, *103*, 14738–14743.
[8] D. P. Galonic, E. W. Barr, C. T. Walsh, J. M. Bollinger Jr., C. Krebs, *Nat. Chem. Biol.* **2007**, *3*, 113–116.
[9] M. Martinho, F. Banse, J.-F. Bartoli, T. A. Mattioli, P. Battioni, O. Horner, S. Bourcier, J.-J. Girerd, *Inorg. Chem.* **2005**, *44*, 9592–9596.
[10] O. Pestovsky, S. Stoian, E. L. Bominaar, X. P. Shan, E. Munck, L. Que Jr., A. Bakac, *Angew. Chem. Int. Ed.* **2005**, *44*, 6871–6874.
[11] J. C. Price, E. W. Barr, T. E. Glass, C. Krebs, J. M. Bollinger Jr., *J. Am. Chem. Soc.* **2003**, *125*, 13008–13009.
[12] J. Kaizer, E. J. Klinker, N. Y. Oh, J. U. Rohde, W. J. Song, A. Stubna, J. Kim, E. Munck, W. Nam, L. Que Jr., *J. Am. Chem. Soc.* **2004**, *126*, 472–473.
[13] A. Decker, J. U. Rohde, L. Que Jr., E. I. Solomon, *J. Am. Chem. Soc.* **2004**, *126*, 5378–5379.
[14] S. Shaik, M. Filatov, D. Schroder, H. Schwarz, *Chem. Eur. J.* **1998**, *4*, 193–199.
[15] H. Hirao, D. Kumar, L. Que Jr., S. Shaik, *J. Am. Chem. Soc.* **2006**, *128*, 8590–8606.
[16] H. Hirao, L. Que Jr., W. Nam, S. Shaik, *Chem. Eur. J.* **2008**, *14*, 1740–1756.
[17] S. Sinnecker, N. Svensen, E. W. Barr, S. Ye, J. M. Bollinger Jr., F. Neese, C. Krebs, *J. Am. Chem. Soc.* **2007**, *129*, 6168–6179.
[18] F. Neese, *J. Biol. Inorg. Chem.* **2006**, *11*, 702–711.
[19] O. Horner, J. M. Mouesca, P. L. Solari, M. Orio, J. L. Oddou, P. Bonville, H. M. Jouve, *J. Biol. Inorg. Chem.* **2007**, *12*, 509–525.
[20] M. H. Lim, J. U. Rohde, A. Stubna, M. R. Bukowski, M. Costas, R. Y. N. Ho, E. Munck, W. Nam, L. Que Jr., *Proc. Natl. Acad. Sci. USA* **2003**, *100*, 3665–3670.
[21] J. F. Berry, E. Bill, E. Bothe, F. Neese, K. Wieghardt, *J. Am. Chem. Soc.* **2006**, *128*, 13515–13528.
[22] A. Sadoc, C. de Graaf, R. Broer, *Phys. Rev. B* **2007**, *75*, 165116.
[23] V. Balland, M. F. Charlot, F. Banse, J. J. Girerd, T. A. Mattioli, E. Bill, J. F. Bartoli, P. Battioni, D. Mansuy, *Eur. J. Inorg. Chem.* **2004**, 301–308.
[24] J. Conradie, I. Wasbotten, A. Ghosh, *J. Inorg. Biochem.* **2006**, *100*, 502–506.
[25] S. Yamamoto, H. Kashiwagi, *Chem. Phys. Lett.* **1988**, *145*, 111–116.
[26] F. Neese, *J. Inorg. Biochem.* **2006**, *100*, 716–726.
[27] E. J. Klinker, J. Kaizer, W. W. Brennessel, N. L. Woodrum, C. J. Cramer, L. Que Jr., *Angew. Chem. Int. Ed.* **2005**, *44*, 3690–3694.
[28] J. U. Rohde, J. H. In, M. H. Lim, W. W. Brennessel, M. R. Bukowski, A. Stubna, E. Munck, W. Nam, L. Que Jr., *Science* **2003**, *299*, 1037–1039.
[29] A. Ghosh, *J. Biol. Inorg. Chem.* **2006**, *11*, 671–673.
[30] M. Verdaguer, A. Bleuzen, V. Marvaud, J. Vaissermann, M. Seuleiman, C. Desplanches, A. Scuiller, C. Train, R. Garde, G. Gelly, C. Lomenech, I. Rosenman, P. Veillet, C. Cartier, F. Villain, *Coord. Chem. Rev.* **1999**, *192*, 1023–1047.
[31] P. Gutlich, A. Hauser, H. Spiering, *Angew. Chem. Int. Ed. Engl.* **1994**, *33*, 2024–2054.
[32] T. H. Dunning Jr., B. H. Botch, J. F. Harrison, *J. Chem. Phys.* **1980**, *72*, 3419.
[33] K. Pierloot, S. Vancoillie, *J. Chem. Phys.* **2006**, *125*, 124303.
[34] H. Bolvin, *J. Phys. Chem. A* **1998**, *102*, 7525.
[35] A. Ghosh, E. Tangen, H. Ryeng, P. R. Taylor, *Eur. J. Inorg. Chem.* **2004**, 4555–4560.
[36] D. Kumar, H. Hirao, L. Que Jr., S. Shaik, *J. Am. Chem. Soc.* **2005**, *127*, 8026–8027.
[37] A. Decker, J. U. Rohde, E. J. Klinker, S. D. Wong, L. Que Jr., E. I. Solomon, *J. Am. Chem. Soc.* **2007**, *129*, 15983–15996.
[38] C. Angeli, R. Cimiraglia, J. P. Malrieu, *J. Chem. Educ.* **2008**, *85*, 150–158.

[39] N. Ben Amor, D. Maynau, *Chem. Phys. Lett.* **1998**, *286*, 211–220.
[40] E. A. Carter, W. A. Goddard III, *J. Phys. Chem.* **1988**, *92*, 2109–2115.
[41] S. Shaik, D. Danovich, A. Fiedler, D. Schroder, H. Schwarz, *Helv. Chim. Acta* **1995**, *78*, 1393–1407.
[42] L. Salem, *Electrons in Chemical Reactions – First Principles*, Wiley-Interscience, **1982**, p. 67–72.
[43] V. Robert, G. Lemercier, *J. Am. Chem. Soc.* **2006**, *128*, 1183–1187.
[44] M. J. Frisch, G. W. Trucks, H. B. Schlegel, G. E. Scuseria, M. A. Robb, J. R. Cheeseman, J. A. Montgomery Jr., T. Vreven, K. N. Kudin, J. C. Burant, J. M. Millam, S. S. Iyengar, J. Tomasi, V. Barone, B. Mennucci, M. Cossi, G. Scalmani, N. Rega, G. A. Petersson, H. Nakatsuji, M. Hada, M. Ehara, K. Toyota, R. Fukuda, J. Hasegawa, M. Ishida, T. Nakajima, Y. Honda, O. Kitao, H. Nakai, M. Klene, X. Li, J. E. Knox, H. P. Hratchian, J. B. Cross, V. Bakken, C. Adamo, J. Jaramillo, R. Gomperts, R. E. Stratmann, O. Yazyev, A. J. Austin, R. Cammi, C. Pomelli, J. W. Ochterski, P. Y. Ayala, K. Morokuma, G. A. Voth, P. Salvador, J. J. Dannenberg, V. G. Zakrzewski, S. Dapprich, A. D. Daniels, M. C. Strain, O. Farkas, D. K. Malick, A. D. Rabuck, K. Raghavachari, J. B. Foresman, J. V. Ortiz, Q. Cui, A. G. Baboul, S. Clifford, J. Cioslowski, B. B. Stefanov, G. Liu, A. Liashenko, P. Piskorz, I. Komaromi, R. L. Martin, D. J. Fox, T. Keith, M. A. Al-Laham, C. Y. Peng, A. Nanayakkara, M. Challacombe, P. M. W. Gill, B. Johnson, W. Chen, M. W. Wong, C. Gonzalez, J. A. Pople, *Gaussian 03*, Revision C.02, Wallingford, CT, **2004**.
[45] K. Anderson, M. P. Fülscher, G. Karlström, R. Lindh, P. A. Malqvist, J. Olsen, B. Roos, A. J. Sadlej, M. R. A. Blomberg, P. E. M. Siegbahn, V. Kello, J. Noga, M. Urban, P. O. Widmark, *MOLCAS (version 5.4)*, University of Lund, Sweden, **1998**.

Received: July 23, 2008
Published Online: September 10, 2008

